

# Contents

<b>1</b>	<b>Introduction</b>	<b>1</b>
<b>2</b>	<b>General approach of the resolution measurement using photon+jet events</b>	<b>1</b>
<b>3</b>	<b>Datasets and event selection</b>	<b>4</b>
3.1	Datasets and triggers . . . . .	4
3.2	Event selection . . . . .	6
<b>4</b>	<b>Methodology of the measurement</b>	<b>9</b>
<b>5</b>	<b>Systematic uncertainties</b>	<b>10</b>
<b>6</b>	<b>Results</b>	<b>10</b>
<b>7</b>	<b>Discussion and conclusion</b>	<b>10</b>



# 1 Introduction

The determination and quantification of the quality of the jet transverse momentum measurement is of crucial interest for many analyses with jet final states, e. g. the measurement of the dijet cross section [1] or  $t\bar{t}$  production cross sections [2]. Also searches for physics beyond the standard model with missing transverse momentum,  $\cancel{p}_T$ , in the final state need a good knowledge of  $\cancel{p}_T$  originating from wrongly measured jets [3–5]. For analyses relying on information from simulation it is very important to correct the simulated resolution to the resolution actually present in data. Therefore, scale factors will be presented to adjust the resolution in simulation to the resolution of the real detector.

In the following sections, a data-based method to measure the jet  $p_T$  resolution in  $\gamma + \text{jet}$  events will be presented. A similar method was already accomplished in earlier analyses [6–9] of 7 TeV data. It is further developed here and applied to 8 TeV data.

The method is based on the transverse momentum balance in the  $\gamma + \text{jet}$  system. It takes advantage of the high resolution of the electromagnetic calorimeter and hence the excellent measurement of the photon energy and momentum. Without initial and final state radiation, the photon and the jet are balanced in the transverse plane. Thus, measuring the photon  $p_T$  with high accuracy leads to an estimate of the true jet transverse momentum offering a possibility to quantify the resolution of jet  $p_T$  measurements.

## 2 General approach of the resolution measurement using photon+jet events

The jet transverse momentum resolution is defined as the standard deviation of the jet transverse momentum response distribution with the response defined as the ratio of the reconstructed to the true jet transverse momentum

$$\mathcal{R} = \frac{p_T^{\text{reco. jet}}}{p_T^{\text{gen. jet}}}. \quad (2.1)$$

The transverse momentum of the generator-level jet is hereby defined as the sum of all particles' transverse momenta that are clustered into the jet cone. It can differ to the

momentum of the original final state quark or gluon by out-of-cone showering effects. Out-of-cone showering refers to particles from the hadronisation process that are not clustered into the jet cone. Throughout the following sections, the jet transverse momentum resolution will be abbreviated JER<sup>1</sup>.

Figure 2.1 shows a typical response distribution for jets in the barrel region. The core of the response distribution shows a Gaussian behavior whereas the tails deviate from that functional form. FIXME: The Gaussian behaviour originates for charged particles contained in the jet, for which the momentum is determined by the curvature of the particles' trajectories, from the distribution of the scattering angle. For neutral particles clustered into a jet, the Gaussian is p and the Poissonian error for neutral hadrons where the momentum is measured with the help of the energy measurement in the calorimeter.

Physical reasons for the low response tail are inter alia semi-leptonic decays of heavy quarks where the neutrino cannot be detected and the reconstructed transverse momentum of the jet is too small (see Fig. 2.1). Only since neutrinos are included into the generator-level jet, this effect is visible. Some instrumental effects, such as a non-linear response of the calorimeter, inhomogeneities of the detector material and electronic noise can contribute to both tails, others, like dead calorimeter channels only contribute to the left tail. The resolution is therefore determined using only the core of the distribution to avoid the coverage of non-Gaussian tails. The resolution is thus defined as the standard

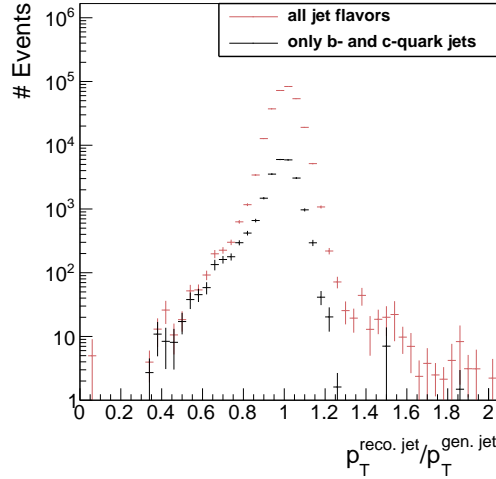


Figure 2.1: Number of events over  $\frac{p_T^{\text{reco. jet}}}{p_T^{\text{gen. jet}}}$  from a simulated  $\gamma + \text{jet}$  sample. The black dots show the contribution by c- and b-quark jets where the left tail originating from semi-leptonic decays of heavy quarks can be seen.

<sup>1</sup>This abbreviation is a historical relic from electron-positron collider experiments where JER referred to jet energy resolution. FIXME - is this correct

deviation of the 99% truncated response histogram divided by the mean of the histogram:

$$\text{JER} = \frac{\sigma_{99\%}}{\mu_{99\%}}.$$

The determination of the 99% range of the histogram is done in several steps. First the mean of the core is found via a Gaussian fit to the histogram in a  $2\sigma$  range<sup>2</sup>. This procedure is done in three iteration steps. Then, a symmetric interval around this mean is determined with its integral equal to 99% of the integral of the full histogram.

The evaluation of the response distribution as reconstructed over generated jet transverse momentum (Eq. (2.1)) is only possible for simulated events where generator-level information is accessible. A determination of the resolution in data, however, has to rely on a different approach.

The main idea of a resolution measurement using  $\gamma$ +jet events is based on the transverse momentum balance of the  $\gamma$  + jet system and the excellent electromagnetic calorimeter resolution (which was estimated between 1.1 % and 3.8% in the barrel region for photons for  $\sqrt{s} = 8$  TeV data [10]).

In Fig 2.2, all tree-level processes contributing to an event topology with one photon and one jet in the final state are depicted. Due to momentum conservation, the jet and the photon are back to back in the transverse plane, and therefore,  $\vec{p}_T^\gamma = -\vec{p}_T^{\text{jet}}$ . Because of the good resolution of the electromagnetic calorimeter, photon energies can be very well measured and thus can serve as an excellent estimator for the true jet energy.

Unfortunately, such clean events are very rare processes, and usually, the momentum balance is spoiled by initial and final state radiation, which lead to further jets in the event (see Fig. 2.3). However, in order to select events that are balanced to a large extent, a lower bound on the angular distance in the transverse plane between the photon and the jet with the highest transverse momentum (leading jet) is required ( $\Delta\Phi > 2.95$  rad).

Additionally, the variable

$$\alpha \doteq \frac{p_T^{2^{\text{nd}} \text{ reco jet}}}{p_T^\gamma}$$

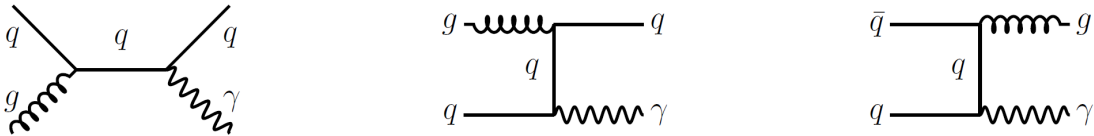


Figure 2.2: Tree-level Feynman diagrams of processes at the LHC in pp collisions with one photon and one jet in the final state.

<sup>2</sup>The  $2\sigma$  range is defined as the range  $[\mu - 2\sigma, \mu + 2\sigma]$ .

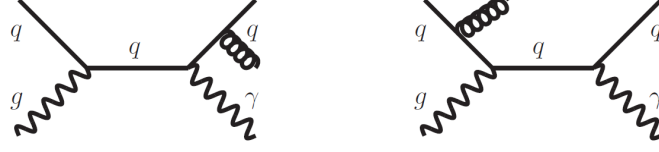


Figure 2.3: Tree-level Feynman diagrams with initial and final state radiation.

is defined as a measure of further jet activity in an event. It is, however, not sufficient to require only an upper bound on  $\alpha$ . Instead, the jet energy resolution is measured in bins of  $\alpha$  (with  $\max(\alpha) = 0.2$ ), and the extrapolated value to zero further jet energy ( $\alpha = 0$ ) is taken as the measured resolution of the jet energy in the absence of further jets.

Measuring the transverse momentum of the photon instead of taking the generator-level jet  $p_T$  leads to the fact that the measured resolution consists out of two parts

$$\frac{p_T^{\text{reco. jet}}}{p_T^\gamma} = \underbrace{\frac{p_T^{\text{reco. jet}}}{p_T^{\text{gen. jet}}}}_{\text{intrinsic}} \cdot \underbrace{\frac{p_T^{\text{gen. jet}}}{p_T^\gamma}}_{\text{imbalance}}.$$

The intrinsic part is the resolution of interest which is independent of further jets in the event whereas the imbalance is strongly dependent on  $\alpha$ .

To extract the intrinsic resolution out of the measured one, the residual imbalance  $q'$  (the imbalance at  $\alpha = 0$ ) is subtracted from the total resolution in the limit of vanishing additional jet activity. As that information is only available from simulation, the measured resolution in data is corrected by the residual imbalance taken from the simulated dataset.

## 3 Datasets and event selection

The measurement of the jet energy resolution is carried out with  $\gamma + \text{jet}$  data recorded during the year 2012 at the CMS experiment. The datasets and triggers that are exploited for this measurement are introduced in the following Section 3.1. In order to select  $\gamma + \text{jet}$  events that are well suited for the resolution measurement, an event selection is applied on top. This event selection is described in Section 3.2.

### 3.1 Datasets and triggers

This analysis exploits several triggers which were active during the year 2012 at the CMS experiment. Because of the high production cross section of  $\gamma + \text{jet}$  events, especially for low

photon  $p_T$ , almost all of these triggers were highly prescaled, i. e. only a fraction of events were actually recorded when the triggers fired. All triggers utilised in this measurement are listed in Table 3.1 together with their recorded luminosity. L1 trigger information

Table 3.1: Single photon triggers together with the recorded luminosity taken the time when they were active and the prescales of the triggers into consideration.

Trigger	Luminosity [ $\text{fb}^{-1}$ ]
HLT_Photon30_CaloIdVL_IsoL	
HLT_Photon50_CaloIdVL_IsoL	
HLT_Photon75_CaloIdVL_IsoL	
HLT_Photon90_CaloIdVL_IsoL	
HLT_Photon135	
HLT_Photon150	

should be described her FIXME. The triggers require a photon with a certain  $p_T$  (as indicated in the name) and, in case of thresholds below 135 GeV also additional quality and isolation criteria. All triggers with threshold below 150 GeV were prescaled.

The events that are selected by the above mentioned triggers are contained in the datasets listed in Table 3.2.

Table 3.2: Single-photon data samples used for the resolution measurement with the contained integrated luminosity.

Dataset	Luminosity [ $\text{fb}^{-1}$ ]
/Photon/Run2012A-22Jan2013-v1/AOD	0.876
/SinglePhoton/Run2012B-22Jan2013-v1/AOD	4.412
/SinglePhoton/Run2012C-22Jan2013-v1/AOD	7.055
/SinglePhotonParked/Run2012D-22Jan2013-v1/AOD	7.354

Monte Carlo simulation data was obtained from a flat PYTHIA6 sample

/G\_Pt-15to3000\_TuneZ2\_Flat\_8TeV\_pythia6/  
 Summer12\_DR53X-PU\_S10\_START53\_V7A-v1/AODSIM

with the events reconstructed with CMSSW\_5.3.2\_patch5 and the Global Tag START53\_V22.

The simulated events were reweighed to match the physical photon  $p_T$  spectrum. Figure 3.1 shows the photon  $p_T$  spectrum in simulation before and after the reweighing. Due to the flat generation, statistical precision remains high, even in the high photon  $p_T$  region.

All simulated samples come with a pileup scenario which does not necessarily match the pileup scenario in data. To match the measured distribution of primary vertices, the events are weighted according to their number of primary vertices. Because almost all of the used triggers are differently prescaled, the distributions of primary vertices differ among the various events triggered by the corresponding trigger. Thus the reweighing has to be done separately for the events falling in the photon  $p_T$  range of the several triggers (see Tab. 3.3). In Fig. 3.2, a comparison between the number of primary vertices for events with  $p_T^\gamma > 165$  GeV is shown before and after the reweighing. For all other triggers the comparison can be found in appendix ??.

### 3.2 Event selection

Events were reconstructed with the particle-flow reconstruction algorithm, which uses information of all detector components to reconstruct individual particles [11]. Furthermore, particles belonging to a jet were clustered with the Anti- $k_t$  jet clustering algorithm with a radius of  $R=0.5$  [?].

To select clean  $\gamma + \text{jet}$  events, it was required that the leading jet meets the following

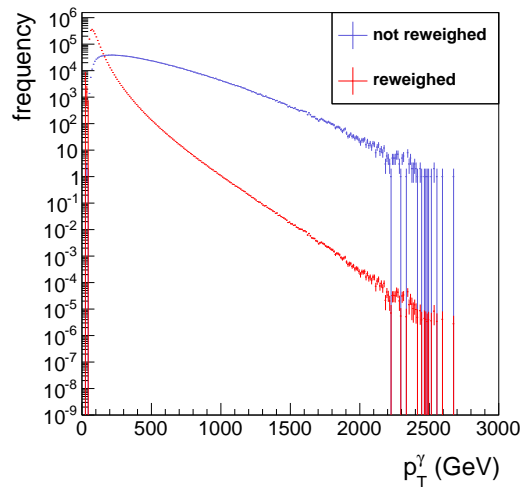


Figure 3.1: The photon  $p_T$  spectrum before (blue) and after (red) reweighing.



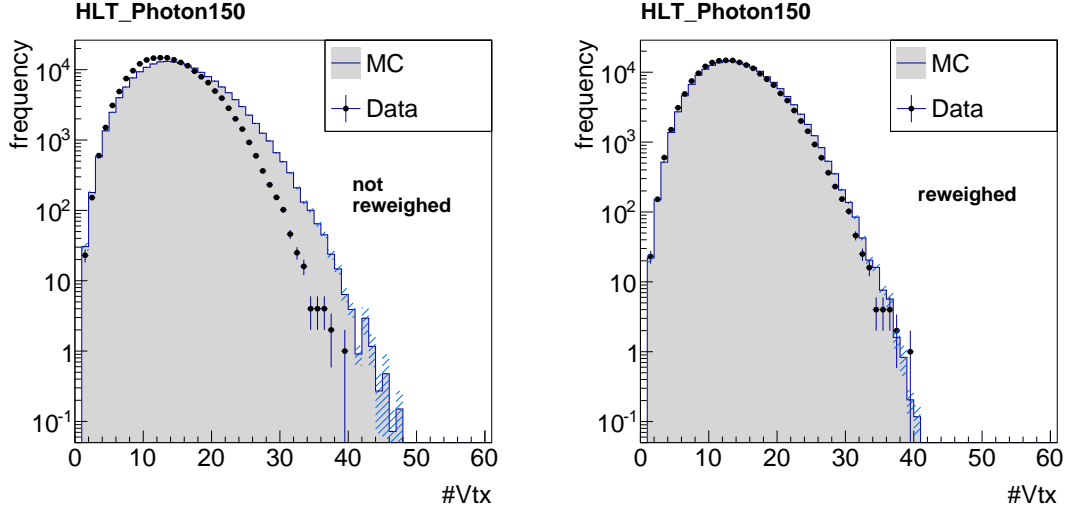


Figure 3.2: The number of primary vertices in data and simulation before (left) and after (right) reweighing for all events with  $p_T^\gamma > 165$  GeV.

requirements (these criteria correspond to a 'tight ID' in [?, ?]):

- Neutral hadron fraction  $< 0.90$
- Neutral electromagnetic fraction  $< 0.90$
- Number of constituents  $> 1$

And for jets in the pseudorapidity range  $|\eta^{\text{jet}}| < 2.4$  :

- Charged hadron fraction  $> 0$
- Charged hadron multiplicity  $> 0$
- Charged electromagnetic fraction  $< 0.99$

To mitigate effects from pileup, the first and second jet were required to have a transverse momentum greater 10 GeV.

Concerning the photon, a maximal pseudorapidity of the photon of  $|\eta^\gamma| < 1.3$  was demanded to exploit the high resolution of the ECAL in the barrel region.

Furthermore, the resolution was determined for different ranges in photon  $p_T$  to avoid mixing of different prescales of the various triggers. In Table 3.3 the applied binning is shown with the respective triggers contributing to each  $p_T^\gamma$  bin.

QCD multijets events constitute an important background to the  $\gamma + \text{jet}$  events: A photon can be faked by a  $\pi^0$  decaying into two close-by photons. Therefore, a very clean selection of the photons is necessary to suppress this background. The following variables were used (see [12] for further explanation of the variables):

Table 3.3: Photon  $p_T$  bins and corresponding triggers.

$p_T^\gamma$ -bins	Trigger
22 GeV	HLT_Photon20_CaloIdVL_IsoL_v*
36 GeV	HLT_Photon30_CaloIdVL_IsoL_v*
60 GeV	HLT_Photon50_CaloIdVL_IsoL_v*
88 GeV	HLT_Photon75_CaloIdVL_IsoL_v*
105 GeV	HLT_Photon90_CaloIdVL_IsoL_v*
149 GeV	HLT_Photon135_v*
165 GeV	HLT_Photon150_v*

- $\frac{H}{E}$  : The ratio of the measured energy in the hadronic calorimeter over the energy measured in the electromagnetic calorimeter. For photons, this is supposed to be very small as they deposit their energy predominantly in the ECAL.
- $\sigma_{i\eta i\eta}$ : The energy weighted spatial width of the photon energy deposition. The electromagnetic shower of a photon has a small lateral size resulting in small  $\sigma_{i\eta i\eta}$  for prompt photons while showers from fake photons, e.g.  $\pi^0 \rightarrow \gamma\gamma$  have a larger lateral size.
- **Jurassic ECAL isolation:** This isolation criterion uses the information of reconstructed hits “RecHits” (coming from the local reconstruction of the digital signals) in a cone around the photon supercluster of  $R=0.4$ . Those are summed up and an upper criterion is identified to discriminate against background which is typically spatially broader.
- **Tower-based HCAL isolation:** The isolation criterion requires the energy deposited in all HCAL towers around the photon in cone of  $R=0.4$  to be small compared to the photon’s energy.
- **Hollow cone track isolation:** Requires absence of high-energetic tracks around the photon.
- **Pixel seed veto:** In order to reduce the background from electrons and positrons, the absence of a pixel-seed in the pixel tracker along the photons trajectory is required.

The upper and lower bounds for the various requirements can be found in table 3.4.

Table 3.4: Upper and lower bounds for all photon isolation criteria in the barrel ( $|\eta^\gamma| < 1.4442$ ).

	Barrel
$\frac{H}{E}$	$< 0.05$
$\sigma_{i\eta i\eta}$	$< 0.013$
ECAL isolation	$< 4.2 + 0.0060 p_T^\gamma$
HCAL isolation	$< 2.2 + 0.0025 p_T^\gamma$
Track Isolation	$< 2.0 + 0.0010 p_T^\gamma$
Pixel seed veto	yes

Besides the mentioned requirements concerning the objects' attributes, two further criteria related to the event topology are crucial for this analysis:

An upper threshold on  $\Delta\Phi$  between the leading jet and the photon and a maximal value for  $\alpha$

- $\Delta\Phi(1\text{st jet}, \gamma) > 2.95\text{rad}$
- $\frac{p_T^{2\text{nd jet}}}{p_T^\gamma} < 0.20$ .

These requirements are important to suppress events with too much further hadronic activity.

A summary of all selection criteria can be found in appendix ??.

Pictures as root file available:

- BLA

Picture **NOT** as root file available:

- BLA

## 4 Methodology of the measurement

- Take from AN

Pictures as root file available:

- BLA

Picture **NOT** as root file available:

- BLA

## 5 Systematic uncertainties

- difficult to take from AN

Pictures as root file available:

- BLA

Picture **NOT** as root file available:

- BLA

## 6 Results

- THINK

Pictures as root file available:

- BLA

Picture **NOT** as root file available:

- BLA

## 7 Discussion and conclusion

- Repeat results

- cross-check analysis
- Outlook

Pictures as root file available:

- BLA

Picture **NOT** as root file available:

- BLA



## Bibliography

- [1] CMS Collaboration, “Measurements of differential dijet cross section in proton-proton collisions at  $\sqrt{s} = 8$  TeV with the CMS detector”, *CMS Physics Analysis Summary* **CMS-PAS-SMP-14-002** (2014).
- [2] CMS Collaboration, “Measurement of the differential cross section for top quark pair production in pp collisions at  $\sqrt{s} = 8$  TeV”, *Eur. Phys. J.* **C75** (2015), no. 11, 542, [arXiv:1505.04480](#). doi:10.1140/epjc/s10052-015-3709-x.
- [3] CMS Collaboration, “Search for new physics in the multijet and missing transverse momentum final state in proton-proton collisions at  $\sqrt{s} = 8$  TeV”, *JHEP* **06** (2014) 055, [arXiv:1402.4770](#). doi:10.1007/JHEP06(2014)055.
- [4] CMS Collaboration, “Searches for Supersymmetry using the  $M_{T2}$  Variable in Hadronic Events Produced in pp Collisions at 8 TeV”, *JHEP* **05** (2015) 078, [arXiv:1502.04358](#). doi:10.1007/JHEP05(2015)078.
- [5] CMS Collaboration, “Search for supersymmetry in hadronic final states with missing transverse energy using the variables  $\alpha_T$  and b-quark multiplicity in pp collisions at  $\sqrt{s} = 8$  TeV”, *Eur. Phys. J.* **C73** (2013), no. 9, 2568, [arXiv:1303.2985](#). doi:10.1140/epjc/s10052-013-2568-6.
- [6] CMS Collaboration, “Determination of Jet Energy Calibration and Transverse Momentum Resolution in CMS”, *JINST* **6** (2011) P11002, [arXiv:1107.4277](#). doi:10.1088/1748-0221/6/11/P11002.
- [7] M. V. F. Pandolfi, D. del Re, “Jet Response and Resolution Measurement with Photon+Jet Events”, *CMS Analysis Note* **CMS-AN-10-076** (2010). Internal documentation.
- [8] F. Pandolfi, D. del Re, M. Voutilainen, “Jet Response and Resolution Measurement with Photon+Jet Events at  $\sqrt{s} = 7$  TeV”, *CMS Analysis Note* **CMS-AN-10-141** (2010). Internal documentation.
- [9] F. Pandolfi, D. del Re, M. Voutilainen, “Update on Jet Response and Resolution Measurements with Photon+Jet Events at  $\sqrt{s} = 7$  TeV”, *CMS Analysis Note* **CMS-AN-10-004** (2011). Internal documentation.

- 
- [10] CMS Collaboration, “Performance of Photon Reconstruction and Identification with the CMS Detector in Proton-Proton Collisions at  $\sqrt{s} = 8$  TeV”, *JINST* **10** (2015), no. 08, P08010, [arXiv:1502.02702](#).  
[doi:10.1088/1748-0221/10/08/P08010](#).
- [11] CMS Collaboration, “Particle-Flow Event Reconstruction in CMS and Performance for Jets, Taus, and  $E_T^{\text{miss}}$ ”, *CMS Physics Analysis Summary* **CMS-PAS-PFT-09-001** (2009).
- [12] CMS Collaboration, “Isolated Photon Reconstruction and Identification at  $\sqrt{s} = 7$  TeV”, *CMS Physics Analysis Summary* **CMS-PAS-EGM-10-006** (2011).



